Process Mapping of Transient Melt Pool Response in Wire Feed E-Beam Additive Manufacturing of Ti-6Al-4V

Jason Fox and Jack Beuth

Department of Mechanical Engineering, Carnegie Mellon University, Pittsburgh, PA 15213

Abstract

Wire feed electron beam additive manufacturing processes are candidates for manufacturing and repair in the aerospace industry. In order to implement feedback or feedforward control approaches, the time needed for a change in process variables to translate into changes in melt pool dimensions is a critical concern. In this research, results from 3D finite element simulations of deposition of Ti-6Al-4V are presented quantifying the transient response of melt pool dimensions to rapid changes in beam power and travel velocity. Results are plotted in beam power vs. beam velocity space, following work by the authors developing P-V Process Maps for steady-state melt pool geometry. Transient responses are determined over a wide range of process variables. Simulation results are compared to initial results from experiments performed at NASA Langley Research Center.

Introduction

Additive Manufacturing (AM) is a layer additive process. In this process, a computer aided drawing (CAD) model is cut into layers. Those layers are used by equipment as build instructions to lay new material on a base substrate or previously added material. Once a part has been built by successive layers, the part can be machined to remove excess material and smooth edges [1].

In AM, both metals and polymers can be used with an electron or laser beam as the heat source and added material can be in wire or powder form. There are several considerations in choosing a focus for this work. Ti-6Al-4V is studied for its use in the aerospace industry, as it is a desirable material in this field due to its strength and corrosion resistance in high temperature applications [2]. There are several advantages to electron beam systems over laser based systems including more efficient energy transfer to the substrate, transfer efficiencies that are not a function of substrate reflectivity, and the ability to deposit a wider range of material systems [3]. Wire feed systems are less complex than powder systems as the powder adds additional variables that must be taken into account (powder density, distribution, and usage efficiency) [1]. For these reasons, this work focuses on Ti-6Al-4V deposition within a wire feed electron beam system.

Background

This research directly addresses wire feed electron beam AM processes (e.g. the EBF3 process developed at NASA Langley or the commercially developed Direct Manufacturing process by Sciaky). Wire feed electron beam AM processes have developed a great demand in the aerospace industry for both repair and production applications. Reduced production and material costs (reduced waste) as well as reduced development and lead time make these very

attractive processes [4]. To help ensure process efficiency, accurate control of the process is required at high deposition rates (high power and velocity), when depositing fine geometries and features (low power and velocity), and transitions in between. Wire feed electron beam AM is performed within a vacuum where an electron beam gun melts the substrate or deposit to create a melt pool. Wire is then fed into the melt pool to deposit a new layer. The positioning system is used to move the substrate and deposit and direct the addition of new material.

Major concerns within the field of AM include microstructure, residual stress, and melt pool size/shape control. Various forms of process maps to understand laser based AM systems were developed by Beuth and Klingbeil [5] and extended by Vasinonta [6] for controlling steady state melt pool size and residual stress in thin-walled and bulky parts. Modeling of residual stress in metal and polymer deposition has also been studied in the work of Klingbeil et al. [7-9] and Ong [10].

Microstructure in laser and electron beam based processes has been studied in several works and is critical for determining part quality. Microstructure evolution in laser based AM has been explored by Kobryn and Semiatin [11], who introduced solidification maps for use in AM. Brandl and Greitemeier [12] examined the effect of heat treatment on the microstructure and hardness of Ti-6Al-4V parts built in AM processes. Bontha et al. [13-15] developed process maps of cooling rates and thermal gradients to predict microstructure. Davis et al. [16] investigated the effect of free edges and process variables (beam power and travel velocity) on melt pool geometry and solidification microstructure (grain size and morphology). Additionally, Gockel and Beuth [17] have identified links between melt pool geometry and microstructure.

The primary reason for controlling melt pool size and shape is to allow a part to be built while maintaining consistent melt pool geometry, even as thermal conditions change. It was shown by Wang et al. [18] that there is a strong dependence of melt pool size and cooling rate on beam power and velocity in LENS™ systems. Advancements to in situ monitoring of the melt pool have been made [19-20]; however, little research has been accomplished to quantify the transient response of the melt pool. The process map approach to controlling melt pool size and shape has been extended to consider transient conditions by Birnbaum et al. [21]. Work by Aggarangsi [22] characterized the transient response of melt pool size for AISI 304 Stainless Steel for small scale (<500W) Laser Engineered Net Shaping (LENS™) systems. Aggarangsi found that melt pool area response could be characterized by distance related to a combination of initial and final steady state melt pool area sizes. Work by Soylemez et al. [3] created a process map for curves of constant melt pool cross sectional area and length-to-depth (L/d) ratios in a process space of 1-5kW and 0-100 in/min for Ti-6Al-4V in EBAM processes.

The purpose of this work is to extend theories of Aggarangsi [22] into the process space defined by Soylemez et al. [3] and test the hypothesis that response times can be predicted based on response distances related to the initial and final steady state melt pool areas in the process space of 1-5kW and 0-100 in/min. The hypothesis is tested through 3D added material finite element simulations of abrupt changes in beam power and beam travel velocity to be run in the ABAQUS™ software package and experiments performed at the NASA Langley Research Center. Through a recent patent [23], the process mapping approach has been generalized to allow transient response in the building of 3-D shapes to be characterized across all direct metal

AM processes and related processes. Those methods extend far beyond those used in the focused study presented herein.

Simulation Methods

The numerical models presented in this work were developed to be run in the ABAQUS™ software package. Three-dimensional finite element simulations have been performed with these models to replicate single bead deposition. The simulation begins with all elements of the model defined and elements representing added material are deactivated. At each step, bead material is reactivated three elements ahead of the heat source. This allows for modeling of the material being added and heat conduction into the wire being fed into the system. The models have an initial temperature of 373K throughout and a constant base temperature of 373K to represent some preheating of the material. Since the process is performed in a vacuum, the models do not contain convection on the outer surfaces. Models also do not include convection within the melted region of the model or losses due to radiation, as these effects are minor compared to conduction through the material. The models include latent heat as well as temperature dependent properties (density, specific heat, and thermal conductivity).

The models are symmetrical along the X-Y face pointing in the positive Z-direction, as seen in Figure 1. They are biased toward the region where material is being added and toward the center of the model in the X direction (region of interest) to reduce computation time. The biased region is sufficiently long to allow the melt pool to reach an initial steady state, induce a step change in beam power or travel velocity, and then reach a new steady state. The models are sufficiently tall, wide, and long to ensure no edge effects are seen in the melt pool. A distributed heat flux is applied to the top surface of the added material to represent the electron beam and mimic rapid oscillation of the beam across the melt pool. The direction of beam travel is in the positive X-direction.
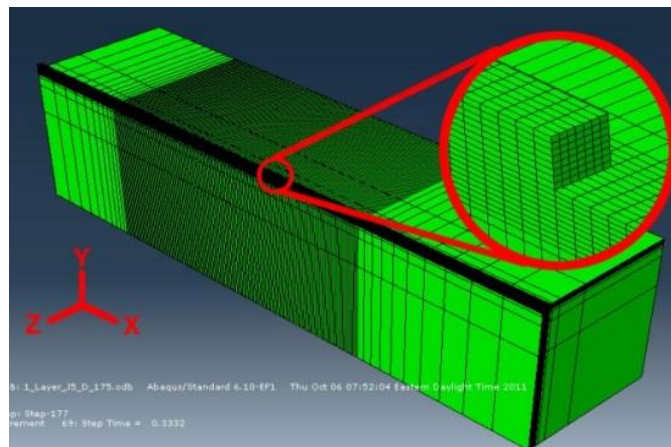

Figure 1. 3D model for finite element simulation using ABAQUS software.

Melt pool area is determined at the point of maximum area, seen in Figure 2. Depth measurements referred to in this work are effective depth based on the maximum cross sectional area, with the area assumed to be semicircular and the depth simply the radius of the cross sectional area.
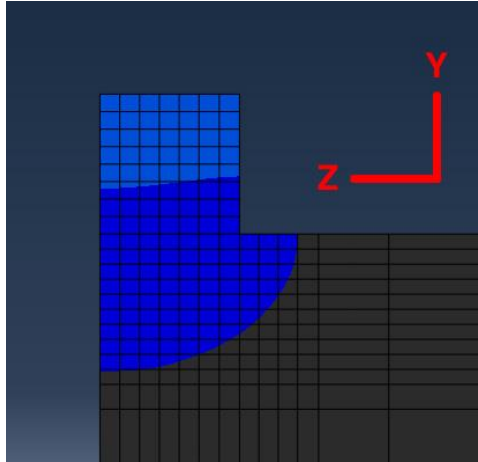
Figure 2. The maximum area of the melt pool as seen from a cut view of the model.

The analysis plan is rooted in the P-V Process Map for single bead geometry previously explored by Soylemez et al. [3], which spans beam powers of 1-5kW and travel velocities of 0-100in/min. The lines of constant melt pool area were determined in the process space. These lines of constant area are represented by solid lines of green, red, and blue (0.063in^2, 0.031in^2, and 0.016in^2 respectively) in Figure 3. The analysis plan, also detailed in Figure 3 and in Table 1, shows step changes analyzed in this work. Step changes in power at constant velocity are represented by vertical dashed lines and step changes in velocity at constant power are represented by horizontal solid yellow and purple lines.
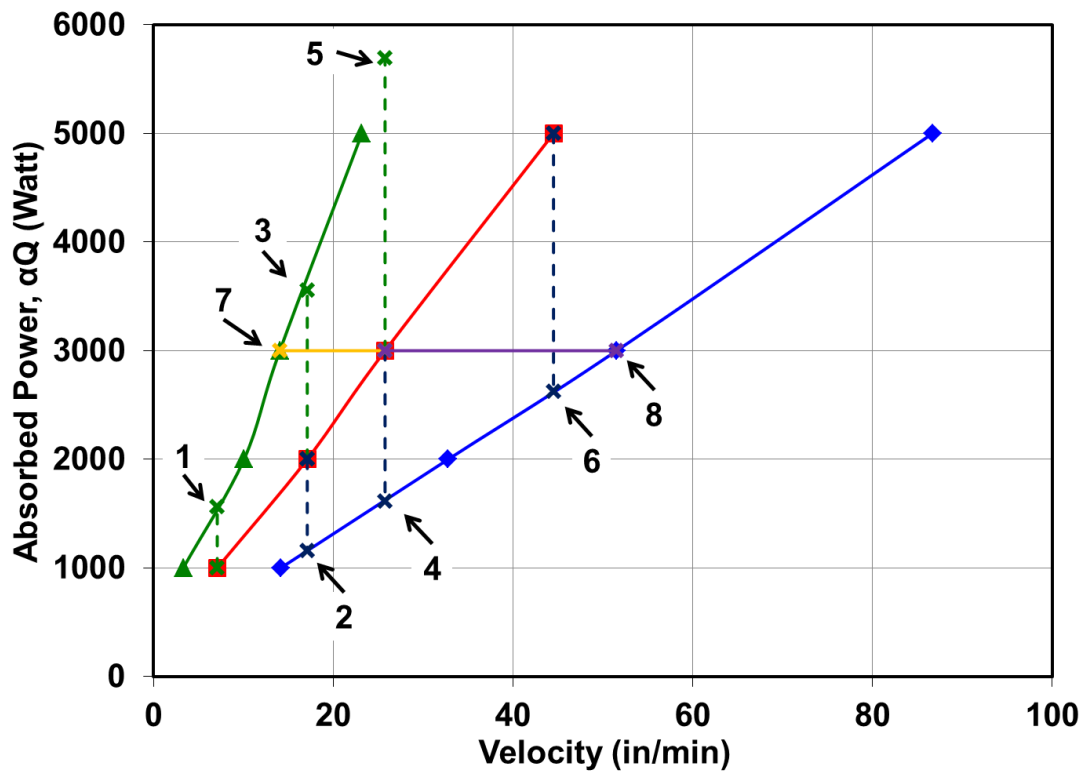

Figure 3. Analysis plan for transient response to step changes in power or velocity.

Run #	Starting Power (W)	Final Power (W)	Starting Velocity (in/min)	Final Velocity (in/min)
1	1559	1000	7.1	7.1
2	1157	2000	17.1	17.1
3	3555	2000	17.1	17.1
4	1614	3000	25.8	25.8
5	5693	3000	25.8	25.8
6	2625	5000	44.5	44.5
7	3000	3000	14.1	25.8
8	3000	3000	51.5	25.8

Table 1. Analysis plan for transient response to step changes in power or velocity.

These step changes were chosen to cover the full process space and jump between the lines of constant area. All step changes end on points on the red constant area line. Lines numbered 1, 3, 5, and 7 are step changes that start on the green line of constant area and decrease in area through decreases in power or increases in velocity to a point on the red line of constant area (Green to Red step changes). Lines numbered 2, 4, 6, and 8 are step changes that start on the blue line of constant area and increase in area through increases in power or decreases in velocity to a point on the red line of constant area (Blue to Red step changes). Lines numbered 1 through 6 are step changes in power at constant velocity and lines numbered 7 and 8 are step changes in velocity at constant power.

Results
3D Finite Element Simulations

In this work, response times are referred to as the time immediately following the step change for the melt pool to reach 90% of the difference between the initial and final steady state depth values. Response distance is referred to as the distance from the initial steady state point of melt pool depth to 90% of the difference between initial and final steady state depth values. Initial and final steady state depths show good agreement with previously determined results [3].

Response times and distances are listed in Table 2. For the response times, there is no clear trend in the values and the times are on the order of seconds. This would represent the limiting factor in a feedback control system as the response times are orders of magnitude longer than the time required for a control system to perform a change in process variables. Response distances, however, group together closely for step changes with matching initial and final steady state melt pool depths. Also, the response distances for the Blue to Red step changes are much shorter than the response distances for Green to Red step changes. Although not shown here, step changes with matching initial and final steady state melt pool effective depths respond similarly as they transition. Thus, response distance is dependent on initial and final melt pool size and response behavior is the same for step changes with matching initial and final steady state depths, regardless of the position or path taken in the P-V Process Map. The explanation for this behavior is that the melt pool must move a certain distance after an abrupt change in beam power

or beam velocity to achieve a new steady-state depth. That distance is largely governed by the initial and final melt pool sizes (melt pool depths or cross sectional areas), regardless of the initial and final power and velocity values.

	Run #	Response Time (s)	Response Distance (in)
Green to Red	1	5.4	0.68
	3	2.4	0.71
	5	1.7	0.67
	7	1.8	0.71
Blue to Red	2	1.9	0.40
	4	1.1	0.43
	6	0.75	0.38
	8	1.2	0.45

Table 2. Response times and response distances from 3D finite element simulations.

Initial Experiments

Initial experiments presented were performed at the NASA Langley Research Center. The experiments did not add material (beam on plate only) and use the same power and velocity combinations as the simulations presented. Tests were performed on a 6in x 12in x 0.25in plate with a distance of approximately ¾ inch from each edge and 0.65 inches between each experiment line. Tests ran for 5.25 inches at the initial power and velocity and 5.25 inches at the final power and velocity to ensure the melt pool had an adequate distance to reach steady state prior to and following the step change in power or velocity.

Figure 4. Experiments performed at NASA Langley Research Center. The top plate contains experiments where the plate returned to room temperature between deposition lines. On the bottom plate, depositions lines were run in rapid succession.

Two sets of experiments were performed. One in which the plate was allowed to return to room temperature between each of the eight experiment lines (Cool Down experiments) and one where the experiments were run in rapid succession (Rapid experiments). An initial comparison of the expected bead width based from simulation results and some of the experiments can be seen in Figure 5. From this result, we see that the expected melt pool width and the response distance match well with the experiment results.
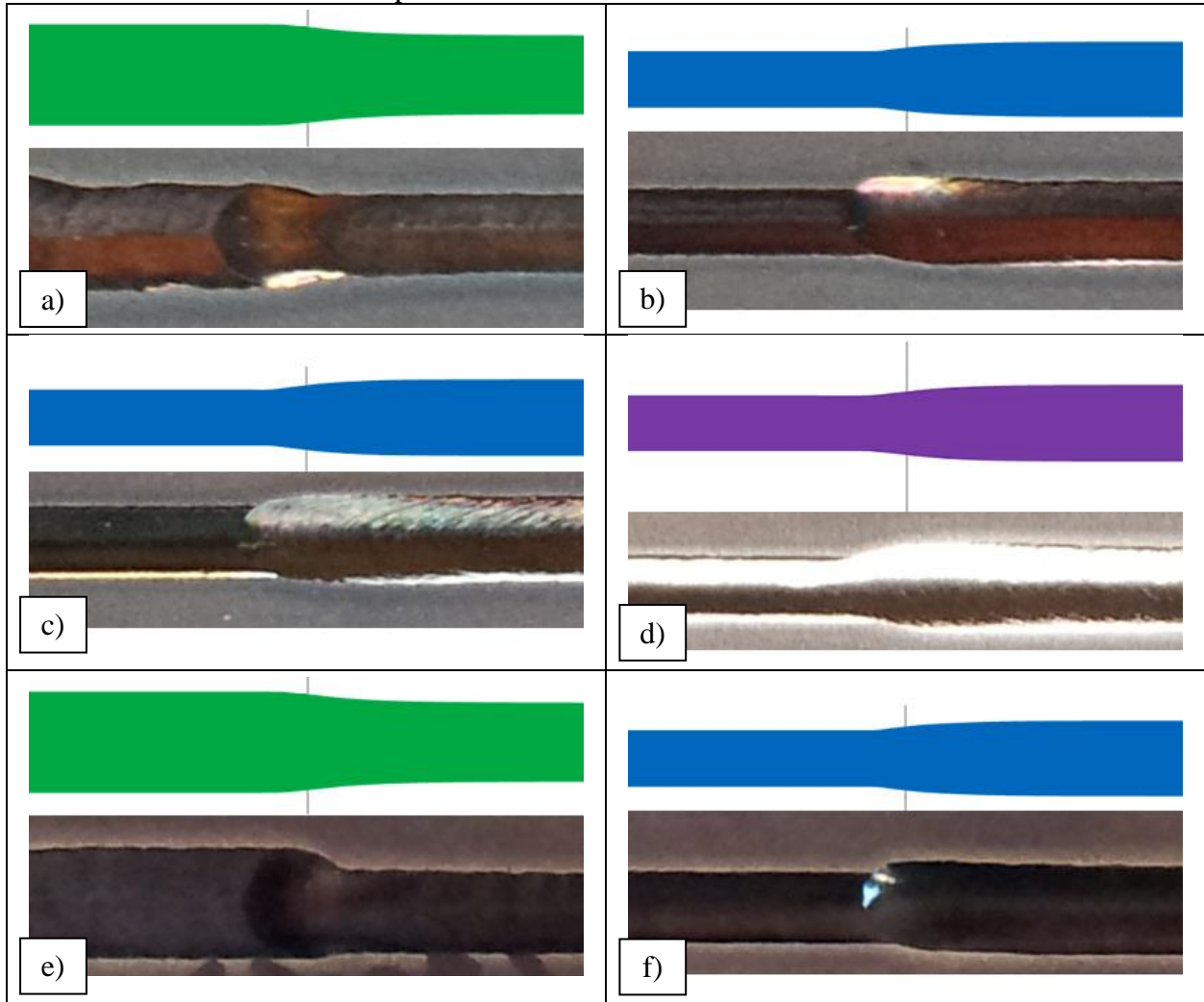

Figure 5. Comparison of melt pool widths seen in simulations versus experiments. Images a) through d) are runs 1, 2, 4, and 8 on the plate allowed to cool to room temperature between depositions and images e) and f) are runs 1 and 2 on the plate where deposition was run in rapid succession.

Conclusions

The goal of this study was to characterize melt pool depth response to step changes in beam power or beam travel velocity for single bead deposition of Ti-6Al-4V over a wide range of powers (1-5kW) and velocities (1-100in/min). This was accomplished through the analysis of 3D finite element simulations. Initial analysis of experiments performed by the NASA Langley

Research Center has shown results consistent with those of the simulations. This study has shown that melt pool response times can be very long (on the order of seconds), which would limit feedback capabilities, and show little correlation or predictable pattern. Response distances, however, show strong similarities when moving between the same lines of constant area. Thus, melt pool depth response does not show dependence on the position or path taken in the P-V Process Map when moving between the same lines of constant area and is instead dependent on initial and final steady state melt pool depths. This can be explained by the melt pool needing to move a certain distance after an abrupt change in beam power or beam velocity to achieve a new steady-state depth. That distance is largely governed by the initial and final melt pool sizes (melt pool depths or cross sectional areas), regardless of the initial and final power and velocity values.

References

[1]   Taminger, K.M., Hafley, R.A. and Dicus, D.L., 2002, "Solid Freeform Fabrication: An Enabling Technology for Future Space Missions," Keynote Lecture for 2002 International Conference on Metal Powder Deposition for Rapid Manufacturing, San Antonio, TX, Metal Powder Industries Federation, April 8-10, 2002, pp. 51-60.

[2]   Taminger, K.M.B. and Hafley, R.A., "Electron Beam Freeform Fabrication: A Rapid Metal Deposition Process," Proceedings of the 3rd Annual Automotive Composites Conference, 2003.

[3]   Soylemez, E., Beuth, J.L. and Taminger, K.M., 2010, "Controlling Melt Pool Dimensions over a Wide Range of Material Deposition Rates in Electron Beam Additive Manufacturing," *Solid Freeform Fabrication Proceedings*, Proc. 2010 Solid Freeform Fabrication Symposium, Austin, pp. 571-582.

[4]   Taminger, K.M. and Hafley, R.A., 2006, "Electron beam freeform fabrication for cost effective near-net shape manufacturing," *NATO/RTOAVT-139 Specialists' Meeting on Cost Effective Manufacture via Net Shape Processing(Amsterdam, the Netherlands, 2006) (NATO)*, pp. 9–25.

[5]   Beuth, J.L. and Klingbeil, N.W., 2001, "The Role of Process Variables in Laser-Based Direct Metal Solid Freeform Fabrication," *JOM,* September 2001, pp. 36-39.

[6]   Vasinonta, A., 2002, "Process Maps for Melt Pool Size and Residual Stress in Laser-based Solid Freeform Fabrication," Ph.D. Thesis, Carnegie Mellon University, May 2002.

[7]   Klingbeil, N.W., Zinn, J.W. and Beuth, J.L., 1997, "Measurement of Residual Stresses in Parts Created by Shape Deposition Manufacturing," *Solid Freeform Fabrication Proceedings*, Proc. 1997 Solid Freeform Fabrication Symposium, Austin, pp. 125-132.

[8]   Klingbeil, N.W., Beuth, J.L., Chin, R.K, and Amon, C.H., 1998, "Measurement and Modeling of Residual Stress-Induced Warping in Direct Metal Deposition Processes,"

Solid Freeform Fabrication Proceedings, Proc. 1998 Solid Freeform Fabrication Symposium, Austin, August 1998, pp. 367-374.

[9] Klingbeil, N.W., Beuth, J.L., Chin, R.K. and Amon, C.H., 2002, "Residual Stress-Induced Warping in Direct Metal Solid Freeform Fabrication," *International Journal of Mechanical Sciences,* Vol. 44, pp. 57-77.

[10] Ong, R., Beuth, J.L. and Weiss, L.E., 2000, "Residual Stress Control Issues for Thermal Deposition of Polymers in SFF Processes," *Solid Freeform Fabrication Proceedings*, Proc. 2000 Solid Freeform Fabrication Symposium, Austin, pp. 209-218.

[11] Kobryn P. A., and Semiatin S. L., 2001, "The laser additive manufacture of Ti-6Al-4V," JOM, **53**(9), pp. 40–42.

[12] Brandl E., and Greitemeier D., 2012, "Microstructure of additive layer manufactured Ti–6Al–4V after exceptional post heat treatments," Materials Letters, **81**, pp. 84–87.

[13] Bontha, S. and Klingbeil, N.W., 2003, "Thermal Process Maps for Controlling Microstructure in Laser-Based Solid Freeform Fabrication," *Solid Freeform Fabrication Proceedings*, Austin, August 2003, pp. 219-226.

[14] Bontha, S., Brown, C., Gaddam, D., Klingbeil, N.W., Kobryn, P.A., Fraser, H.L., and Sears, J.W., 2004, "Effects of Process Variables and Size Scale on Solidification Microstructure in Laser-Based Solid Freeform Fabrication of Ti-6Al-4V," *Solid Freeform Fabrication Proceedings*, Austin, August 2004.

[15] Bontha, S., Klingbeil, N.W., Kobryn, P.A. and Frasier, H.L., 2009, "Effects of Process Variables and Size-Scale on Solidification Microstructure in Beam-Based Fabrication of Bulky 3D Structures," *Material Science and Engineering A*, Vol. 513-514, pp. 311-318.

[16] Davis, J.E., Klingbeil, N.W. and Bontha, S., 2010, "Effect of Free-Edges on Melt Pool Geometry and Solidification Microstructure in Beam-Based Fabrication of Bulky 3-D Structures," *Solid Freeform Fabrication Proceedings*, Proc. 2010 Solid Freeform Fabrication Symposium, Austin, pp. 230-241.

[17] Gockel, J.E. and Beuth, J.L., "Understanding Ti-6Al-4V Microstructure Control in Additive Manufacturing via Process Maps," *Solid Freeform Fabrication Proceedings*, Austin, August 2013 (in the current proceedings).

[18] Wang, L., Felicelli, S., Gooroochurn, Y., Wang, P. T. and Horstemeyer, M.F., 2008, "Optimization of the LENS process for Steady Molten Pool Size," *Materials Science and Engineering A,* Vol. 474, No. 1-2, pp. 148-156.

[19] Song L., and Mazumder J., 2011, "Feedback Control of Melt Pool Temperature During Laser Cladding Process," IEEE Transactions on Control Systems Technology, **19**(6), pp. 1349–1356.

[20] Song L., Bagavath-Singh V., Dutta B., and Mazumder J., 2012, "Control of melt pool temperature and deposition height during direct metal deposition process," Int J Adv Manuf Technol, **58**(1-4), pp. 247–256.

[21] Birnbaum, A., Aggarangsi, P. and Beuth, J.L., 2003, "Process Scaling and Transient Melt Pool Size Control in Laser-Based Additive Manufacturing Processes," *Solid Freeform Fabrication Proceedings*, Austin, August 2003, pp. 328-339.

[22] Aggarangsi, P., 2006, "Transient Melt Pool Size and Stress Control in Additive Manufacturing Processes," PhD Thesis, Carnegie Mellon University.

[23] Beuth, J., and Fox, J., "Process Mapping of Thermal Response Due to Process Variable Changes," Provisional Patent, filed March 15, 2013.